Dft and Td-Dft Study of Triazavirin Drug Derivatives as Antiviral to Coronavirus Covid-19

Husam A. Naser[1]*, Samar M. Merdas[1], Falah H. Hanoon[1],[2], Alaa N. Hussien[3]
[1]Department of physics, College of Science, University of Thi Qar, Nassiriya 64000, IRAQ.
[2]National University of Science and Technology, Nassiriya 64000, IRAQ.
[3]Department of Mechanical Techniques, Al-Nassiriya Technical Institute, Southern Technical University, Nassiriya 64000, IRAQ.
Email: husamalaa997@gmail.com

Abstract
A global health pandemic that began in December 2019 was the new SARS-CoV-19 coronavirus. The bioactivities of the heterocyclic drug triazavirin selected have been assessed in this study using computer modelling strategies as inhibitors and nucleotide analogs for COVID-19. Triazavirin is an antiviral drug that is synthesized with triazavirin (2-methylsulfanyl-6-nitro[1,2,4]triazolo[5,1-C][1,2,4]triazine-7(4H)-one, TZV). For potential requirements against the 2019-nCoV Coronavirus, TZV is being investigated. We have conducted a computerized study for the screening of effective Triazavirin (C 5H4N6O3S) available medication which can be inhibitors for the Mpro of 2019-nCoV in order to find candidate drugs for the 2019-nCoV period. In the present work, (DFT/TD-DFT/B3LYP/6-31G(d,p)) calculations have been carried out first of all for the purposes of estimating the thermal parameters, dipole momentum, polarization, and molecular power of the drug currently in the gas stage of the molecular structure of the title molecules. The studied compound has also calculated and shown its molecular HOMO-LUMO, its excitation energy, and its oscillator strengths. DFT and TD-DFT studies have been conducted to interact the TZV compound with the Coronavirus. Thus, TZV can be applied for possible application against Coronavirus 2019-nCoV applications.
Keywords: Coronavirus disease 2019; SARS-COV-2; Triazavirin drug; DFT; TD-DFT; electronic properties.

1. Introduction

From the late of year 2019, novel coronavirus disease (COVID-19) has been spread almost all around the world and made several serious problems to the public health [1]. Without any available approved antiviral, several attempts have been dedicated to explore medicinal compounds for supportive care of this infection [2]. In addition to explore novel compounds, examining available drugs is an important task to rapid detection of a way for pharmacotherapy of COVID-19. By introducing protease structure of COVID-19 in the early of year 2020 [3], considerable efforts have been done to examine the efficacy of available related drugs on the enzymatic activity [4]. Novel coronavirus (COVID 19) has been infected and spread speedily all over the world and is transferred primarily through contact with infected saliva droplets or nose release when infected individuals cough or sneeze. Human coronaviruses were primarily identified in the mid-1960s [5-7].

A novel coronavirus, formerly known as the 2019 new coronavirus(2019-nCoV), was found in Wuhan, China in December 2019, and was sequenced and isolated by January 2020 [8]. In December 2019 a novel coronavirus was found in the Wuhan province of China. The disease, now known as the COVID-19 disease, has spread rapidly throughout China, infecting many more persons causing economic and social paralysis in the world. On 16 May 2020, almost 4.5 million laboratory-confirmed infections, including over 300,000 deaths, were reported worldwide [9]. Studies have close relationship to SARS-CoV-1 and SARS-CoV-2 and show that genes of SARS-CoV-2 share >80% of nucleotides, with 89,1% of the nucleotides of SARS-CoV genes. Severe acute respiratory syndrome (SARS-CoV) [10], the 2019-nCoV virus, a mutant lineage β beta-coronavirus, uses the human cell angiotensin transforming enzyme2 (ACE2) as a receptor. Coronavirus has the greatest protein envelope of viral positive stranded RNA [11]. The SARS-CoV maturation process is streamed through polyprotein protein cleavage which affects the virus' replication and transcript. The principal enzyme in this event is CoV protease (CoV Mpro). Protein inhibition is an appealing coronavirus management strategy. Any gene mutations corresponding to CoV Mpro can produce their variety of mutants that are partial or completely resistant to these compounds. In order to fight such rapid mutation-capable viruses it is very essential to develop new anti-SARC-CoV-2 Mpro [12].

The various existing drugs, including triazavirin, have been reported to show potential resistance to COVID-19 (TZV). Because most of the medicines are inhibitors of HIV protease. Triazavirin has also been reported to have shown anti-SARS-CoV-1 effect, due to depletion of angiotensin-conversion enzyme glycosylation 2 (ACE2) [4]. At low pH, this medicine is further enhanced by interfering in viral protease and glycosyl transmission post-translation

doi.org/10.31838/hiv23.02.177 Received: 05.10.22, Revised: 02.11.22, Accepted: 04.12.22

modifications in the reticular endoplasm or trans Golgi complex vesicles. Consequently, triazavirin has been docked with COVID-19 principal protease as well [13-15].

Since 2015, triazavirin (TZV), a new antiviral medicinal product, was launched in Russia. It is analogous to the purine nucleoside bases in synthetic form. TZV's main mode of action inhibits viral RNA synthesis and avoids genomic fragments replication. TZV has a widespread range of antiviral activities against RNA-containing viruses, including influenza A virus (H5N1), influenza B virus, tick-borne encephalitis, and forest-Spring encephalitis, both in vitro and in vivo animal models [16-18], due to its multifarious action mechanism. The recommended dose of TZV is 250 mg three times daily for a consistent 5–7 d according to the package insert. The consequences showed that TZV can substantially reduce the period of main clinical symptoms of the influenza and reduce the incidence of influenza-related complications and complications caused by the concurrence use of symptomatic medicines, and the patient received 250 mg TZV orally three-fold in phase II on TZV with 5 d. There have been no reported clear adverse events (AEs) [19-21]. However, up to the anticipated positive consequences of RCT are obtained from TZV, the effectiveness and safety of COVID-19 remain uncertain. Therefore, in order to test TZV effectiveness and safety for COVID-19, we have established the present multicenter and blind RCT. In this study, We have performed DFT and TD-DFT calculations to investigate the undertake a systematic theoretical study of unsubstituted triazavirin and substituting hydrogen of TZV by other halogens namely fluorine, chlorine, bromine, cyanide group and the hydroxyl group. We investigated these compounds in terms of their structural and spectroscopic parameters by using Gaussian 09W program [22].

2. Result and Discussion

2.1 Quantum mechanics calculations

All of quantum calculations in this study were carried out using regular Gaussian 09W program. The DFT computations have been done in gas phase by means of DFT method with B3LYP/ 6-31G(d,p) basis set. set. All optimum compounds (**Fig. 1**) are stable, and this is approved in terms of the absence of the imaginary frequency. The theoretical geometrical parameters of TZV are summarized in **Table 1**. The results of the theoretical density functional theory calculations for all investigated drugs revealed the non-planarity except for compound **TZV**. The estimated DFT calculations for thermal parameters, dipole moment and the polarizability of the drug derivatives are collected in **Table 2**. These structural parameters will be useful when these compounds are synthesized and characterized[23].

Taple 1. Bond lengths (A°), bond angles (°) and dihedral angles (°) results for the triazavirin drug by using DFT B3LYP/6-31G (d,p)

Bond lengths (A°)	Computed	Bond angles (°)	Computed	Dihedral angles (°)	Computed
C1-C2	1.5375	C2-C1-N6	114.17	N6-C1-C2-N3	0.0
C1-N6	1.4415	C2-C1-O15	122.91	N6-C1-C2-N9	180.0
C1-O15	1.2584	N6-C1-O15	122.92	O15-C1-C2-N3	180.0
C2-N3	1.3186	C1-C2-N3	119.48	O15-C1-C2-N9	0.0
C2-N9	1.47	C1-C2-N9	120.26	C2-C1-N6-C5	0.0
N3-N4	1.4279	N3-C2-N9	120.26	C2-C1-N6-N7	180.0
N4-C5	1.2975	C2-N3-N4	123.07	O15-C1-N6-C5	180.0
C5-N6	1.4236	N3-N4-C5	120.19	O15-C1-N6-N7	0.0
C5-N8	1.4763	N4-C5-N6	122.54	C1-C2-N3-N4	0.0
N6-N7	1.3792	N4-C5-N8	129.02	N9-C2-N3-N4	180.0
N7-C10	1.481	N6-C5-N8	108.44	C1-C2-N9-O13	0.0
N7-H19	1.0	C1-N6-C5	120.55	C1-C2-N9-O14	180.0
N8-C10	1.3209	C1-N6-N7	131.79	N3-C2-N9-O13	180.0
N9-O13	1.36	C5-N6-N7	107.67	N3-C2-N9-O14	0.0
N9-O14	1.1968	N6-N7-C10	106.73	C2-N3-N4-C5	0.0
C10-S11	1.78	N6-N7-H19	126.63	N3-N4-C5-N6	0.0
S11-C12	1.78	C10-N7-H19	126.63	N3-N4-C5-N8	180.0
C12-H16A	1.07	C5-N8-C10	106.17	N4-C5-N6-C1	0.0
C12-H17B	1.07	C2-N9-O13	120.0	N4-C5-N6-N7	180.0
C12-H18C	1.07	C2-N9-O14	120.0	N8-C5-N6-C1	180.0
		O13-N9-O14	120.0	N8-C5-N6-N7	0.0
		N7-C10-N8	110.98	N4-C5-N8-C10	180.0
		N7-C10-S11	124.51	N6-C5-N8-C10	0.0
		N8-C10-S11	124.51	C1-N6-N7-C10	180.0
		C10-S11-C12	109.47	C1-N6-N7-H19	0.0
		S11-C12-H16A	90.0	C5-N6-N7-C10	0.0
		S11-C12-H17B	144.74	C5-N6-N7-H19	180.0
		S11-C12-H18C	125.26	N6-N7-C10-N8	0.0
		H16A-C12-H17B	54.74	N6-N7-C10-S11	180.0
		H16A-C12-H18C	144.74	H19-N7-C10-N8	180.0
		H17B-C12-H18C	90.0	H19-N7-C10-S11	0.0
				C5-N8-C10-N7	0.0
				C5-N8-C10-S11	180.0
				N7-C10-S11-C12	180.0
				N8-C10-S11-C12	0.0
				C10-S11-C12-H16A	180.0
				C10-S11-C12-H17B	180.0
				C10-S11-C12-H18C	0.0

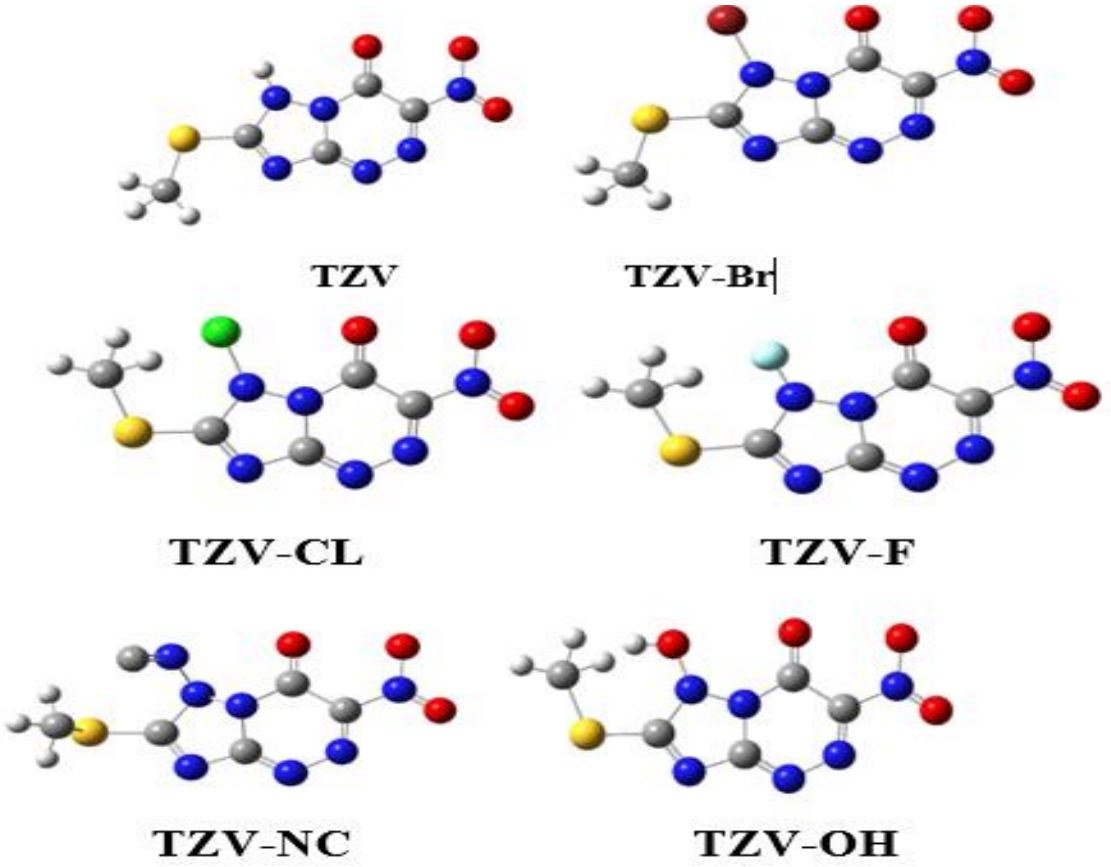

Figure 1. Enhanced geometrical configurations of present compounds.

Table 2. Thermal parameters (Hartree/Particle), polarizability ($Bohr^3$) and dipole moment (Debye) of drugs.

Drugs	Ecorr	ZPVE	Etotal	H	G	DM	α
TZV	0.102	- 1144.72	- 1144.71	- 1144.71	- 1144.76	13.56	148.89
TZV-Br	0.092	- 3715.79	- 3715.77	- 3715.77	- 3715.82	13.34	168.37
TZV-CL	0.093	- 1604.25	- 1604.23	- 1604.23	- 1604.28	10.07	165.24
TZV-F	0.094	- 1243.85	- 1243.84	- 1243.84	- 1243.89	10.21	153.52
TZV-NC	0.096	- 1236.82	- 1236.81	- 1236.81	- 1236.86	10.20	153.52
TZV-OH	0.106	- 1219.78	- 1219.77	- 1219.77	- 1219.82	11.52	150.49

ZPVE: Sum of zero-point and electronic energies; Etotal: Sum of thermal and electronic energies; H: Sum of electronic and thermal enthalpies; G: Sum of electronic and thermal free energies; DM: dipole moment; α: polarization[24].

The DFT estimated data revealed that the dipole moment of the drugs under investigation is in the order of TZV < TZV-Br < TZV-OH < TZV-F < TZV-NC < TZV-Cl. The high dipole moment TZV could show its binding role within a particular target protein and its binding energy consequences, which will be discussed based on Gaussian 09W software. The materials' polarization depends on how the sensitivity of the cloud of electron molecular systems affects a load approach. In addition, it depends on the compound complexity and the molecular structure size. The smallest compound TZV, with the least polarizability (148.89$bohr^3$) is noticed, however the most complex drug TZV-Br (168.24 $bohr^3$) is predicted to be highly polarized with 168.24 $bohr^3$. The dipole moments of the drugs examined are calculated to be between 13.56 and 10.07 Debye in the order of TZV > TZV-Br > TZV-OH > TZV-F > TZV-NC > TZV-CL, are tabulated in Table 2.

2.1.1. Frontier molecular orbitals

Frontier molecular orbitals (FMOs) stand for highest occupied molecular orbital (HOMO) and the least unoccupied molecular orbital (LUMO). The HOMO stands for the highest-energy orbital that is equipped with electrons. Consequently, it is an electric donor, and LUMO is the lowest-energy orbital with an electron-acceptor space. These orbitals control the mode of drug interaction with other molecules as in their receptor-to-drug interactions. The FMO may provide realistic, qualitative information on the sensitivity of HOMO electrons to LUMO. For triazavirin derivatives, the energy levels and the LUMO-HOMO gap are measured as shown in Fig. 2. In addition, HOMO and LUMO have been significant quantum chemical parameters for determining the molecular reactivity and are employed for calculating numerous imperative parameters, involving descriptors of chemical reactivity. The HOMO and LUMO energies of the compounds studied were calculated using the DFT method set in B3LYP/ 6-31G (d,p) and Table 3. HOMO and LUMO isodensity plots are illustrated in Fig. 3 for the compounds investigated. The green

color represents the negative phase; on the other hand the red color corresponds to the positive phase which is well clarified in the density of states (DOS) spectrum (Fig. 4). DOS spectrums characterize the energy levels per unit energy increment and its composing in energy. The displaying study per orbital shows that the green and the red lines in these curves correspond to the HOMO and LUMO energy levels, respectively.

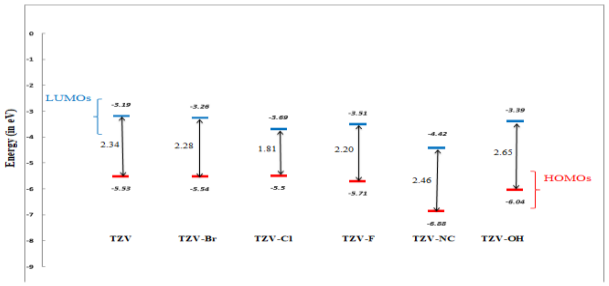

Figure 2. The computed energy levels and LUMO-HOMO gap for triazavirin derivatives.

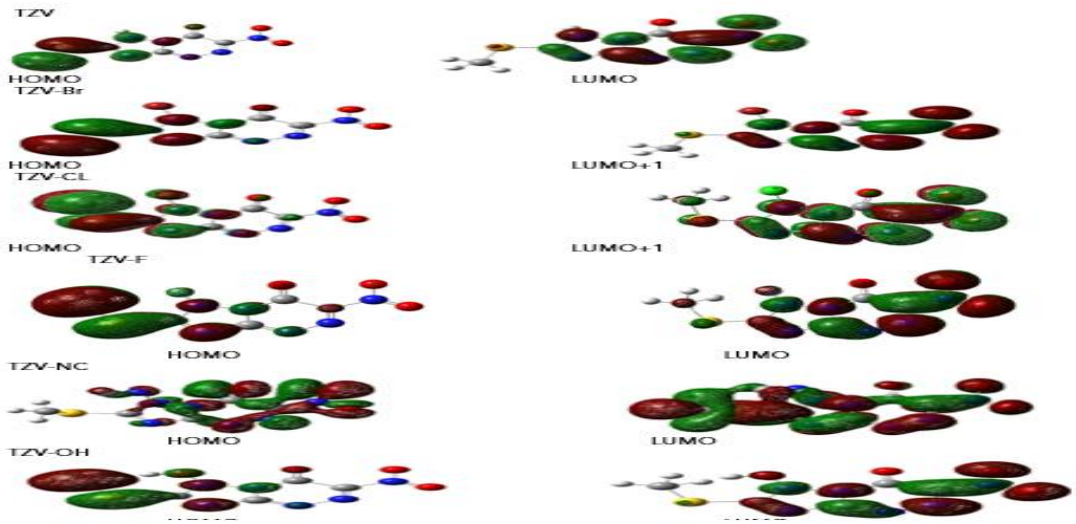

Figure 3. The LUMO and HOMO distribution patterns.

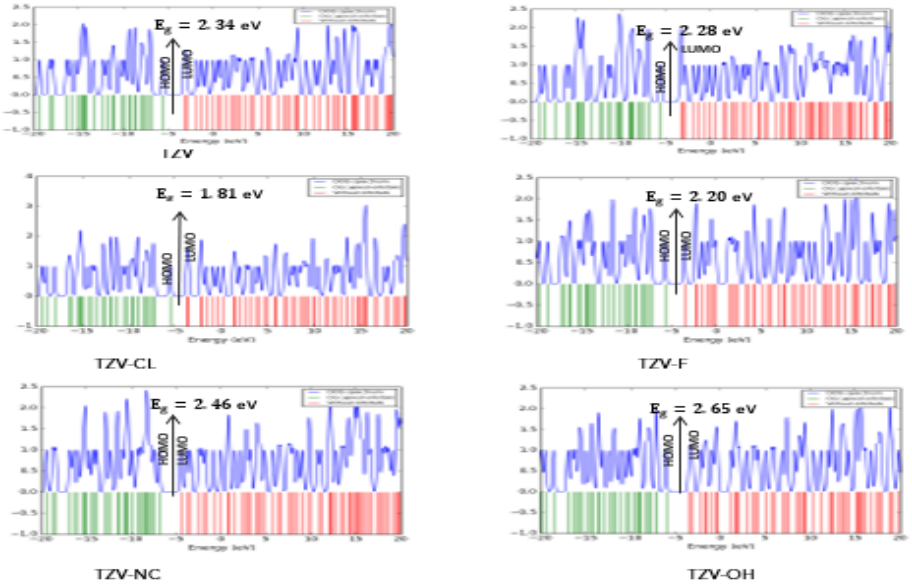

Figure 4. The dependence of density of states versus incident electron energy for (TZV - TZV-OH) drugs.

The consequences of the energy analysis for FMOs have shown that TZV-NC drug HOMO energies are lower than the other compounds. However, LUMO level destabilization in TZV-NC is higher than in the other. Accordingly, TZV-CL < TZV-F< TZV-Br < TZV< TZV-NC< TZV-OH is the energy gap in the considered drugs.

Table 3. HOMO and LUMO energy values (eV) of the compounds studied.

Drugs	HOMO	HOMO-1	LUMO	LUMO+1	Eg
TZV	-5.53	-6.94	-3.19	-2.95	2.34
TZV-Br	-5.54	-6.91	-3.26	-3.23	2.28
TZV-CL	-5.50	-7.24	-3.69	-3.52	1.81
TZV-F	-5.71	-7.23	-3.51	-2.31	2.20
TZV-NC	-6.88	-7.42	-4.42	-3.80	2.46
TZV-OH	-6.04	-7.04	-3.39	-3.10	2.65

The DFT estimates for frontier molecular orbitals on the other hand showed their effect on the bioactive characteristics of these compounds by comparing the energy level of HOMO and LUMO and their energy gap of the medicinal products investigated. However, dependent upon the conjugation and the nature, the HOMOs have a range of energy levels ranging from – 5.50 eV to – 6.88 eV; the LUMOs are however between – 3.19 eV and – 4.42 eV. Furthermore, for TZV, TZV-CL, TZV-Br, TZV-F, TZV-NC and TZV-OH the energy gap order has been 2.34, 1.81, 2.28, 2.20, 2.46 and 2.65 eV, respectively. It is obvious that the high-lying HOMO TZV-CL drug is the most likely electron donor are tabulated in Table 3.

Many reports have shown recently that the structural activity relationships of FMOs should be taken into account in the study. The theory of FMOs has shown the most important aspect of bioactivity of small structural pharmaceutical drugs is their energy level. However, LUMOs primarily accept electrons, offering electrons. Obviously, for all drugs investigated the energy level of HOMOs is different. Compound TZV-CL showed the HOMO most lying and could thus be a better electron donor drug than other drugs. Of note are several hydrophilic interactions, TZV-OH drug with the biggest energy gap Eg=2.65 eV that could facilitate connection with the receptors. This indicates that such hydrophilic interactions have a significant impact on the receptionist affinity of such small drugs. During the binding process the HOMO of a certain drug and the LUMO could be shared with the adjacent residue. The binding energy of compounds TZV – TZV-OH ranged between 0.392 to 1.215 eV as presented in Table 4.

Table 4. Estimated binding energy (in eV) for triazavirin derivatives.

Drugs	Binding energy (eV)
TZV	1.209
TZV-Br	1.215
TZV-CL	1.01
TZV-F	0.392
TZV-NC	1.153
TZV-OH	1.207

2.1.2. Quantum chemical calculations

Indicators of ionizing potential (I= -EHOMO) and electron affinity (A= - ELUMO) of molecules are EHOMO and ELUMO. Other descriptors of the chemical reactivity, chemical hardness (η), electronegativity (χ), chemical softness (δ), chemical potential (μ), electrophilicity index (ω) and maximum charge transfer index (ΔNmax) are used as well as the frontier molecular orbitals. The following equations have been adopted in calculations as follows [25, 26]:

$\eta = (I-A)/2$ (1)

$\chi = (I+A)/2$ (2)

$\delta = 1/2\eta$ (3)

$\mu = -(I+A)/2$ (4)

$\omega = \mu^2/2\eta$ (5)

$\Delta N_{max} = -\mu/\eta$ (6)

The χ value is a forecast of the molecule's power to attract electron, e.g., lewis acid, whereas small value (χ) is a good base. Global hardness (η) stands for a degree of prohibition against charging, but global softness (δ) marks the ability to accept electrons for a molecule [25]. Soft molecules have a small energy gap between molecular frontier orbitals and are more reactive than the harder, as electrons could be transferred to the accepters easily. Electrophilicity is an indicator of the lower energy differences based on the highest electron movement between LUMO and HOMO as accepter and donor respectively.

Table 5. Calculated of some glopal reactivity descriptors of triazavirin derivatives.

Drugs	I	A	η	χ	δ	μ	ω	ΔNmax
TZV	5.53	3.19	1.17	4.36	0.427	- 4.36	8.124	3.726
TZV-Br	5.54	3.23	1.14	4.40	0.439	- 4.40	8.491	3.859
TZV-CL	5.50	3.52	0.91	4.60	0.549	- 4.60	11.626	5.055
TZV-F	5.71	3.51	1.10	4.61	0.455	- 4.61	9.660	4.191
TZV-NC	6.88	4.42	1.23	5.65	0.407	- 5.65	12.977	4.593
TZV-OH	6.04	3.39	1.33	4.72	0.376	- 4.72	8.375	3.549

Using the energies of FMOs, we calculated the reactivity descriptors of triazavirin derivatives molecules. A= - E_{LUMO}: represent the electron affinity; I = - E_{HOMO} represent the ionization potential and μ = -(I+A)/2 is the electronic chemical potential. The chemical hardness (η) are between 0.91 to 1.33 eV for **TZV – TZV-OH** drugs, respectively. The chemical softness (δ) has been computed and found to be 0.376 to 0.549 eV^{-1}. Moreover, the electrophilicity index (ω) is about 8.124 to 12.977 eV for triazavirin derivatives. Based on the value found of the electrophilicity index, we can conclude that the **TZV-NC** is a good electrophile better than triazavirin derivatives. Therefore, it is able to accept an electron doublet in order to form bonds with another reagent which is necessarily a nucleophile. Electronegativity is also determined χ = (I+A)/2 and it is found to be 4.36 to 5.65 eV.

2.1.3. Molecular Electrostatic Potential (MEP)

The molecular electrostatic potential (MEP) is

important for computing and validating the evidence on a reactivity of a drug as inhibitors. Although the MEP gives a sign of the molecular size and form of the positive, negative and neutral power. This might be a tool for predicting the physicochemical properties of the drug under investigation in relation to the molecular structure. In addition, a useful tool to assess drug reactivity towards electrophilic and nuclear attacks is the Molecular Electrostatic Potential.

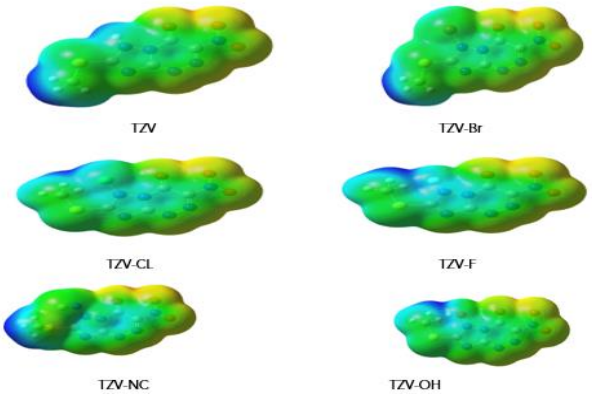

Figure 5. Molecular electrostatic potentials (MEP) of drugs.

The electrostatic molecular potential of the medicines studied (**TZV – TZV-OH**) is determined using the same method in the same basis sets in **Fig. 5**. The MEPs prefer electrophilic attack locations to be the lowest negative region, shown as red. The negatively charged sites and the opposite satiation for the blue regions will thus attract an attacking electrophile. Obviously, because of the nature of atoms, their electronic nature, the molecular size and shape and the orientation of the negative, positive and neutral electrostatic potential vary according to the drug. The main cause for variation in its bonding affinity to the activity site receptor could be the difference in mapping the electrostatic potential around a drug.

2.1.4. Mulliken Atomic Charges

The Mulliken atomic charges of the estimated drugs were calculated by DFT using B3LYP at 6-31G (d,p) as a method basis set, the data were tabulated in Table 6. It showed that the C5 is the most positive and C12 have the most negative charge for TZV drug. On the other hand, it is observed that the most nucleophilic centers of TZV-Br drug are N3 and N9 which are the most electrophilic susceptibility positions. On the other hand, it is obvious that the nucleophilic susceptibility of the TZV-CL drug is recognized on C5 and C10 sites. However, N9 and N10 are the most negative charges of TZV-F, TZV-NC and TZV-OH drugs and their respective positively charged atoms are C5 and C6. The positively charged centers are the most susceptible sites for nucleophilic attacks i.e., electron donation. However, the most negatively charged centers are the most susceptible sites for electrophilic one.

Table 6. Mulliken atomic charges of the estimated drugs.

TZV	TZV-Br	TZV-CL	TZV-F	TZV-NC	TZV-OH
1 C 0.6112	1 C 0.4471	1 C 0.4471	1 C 0.6183	1 C 0.5921	1 C 0.6242
2 C 0.4412	2 N - 0.2885	2 N - 0.2836	2 C 0.4464	2 C 0.4821	2 C 0.4438
3 N - 0.2891	3 N - 0.3853	3 N - 0.3769	3 N - 0.2836	3 N - 0.2789	3 N - 0.2862
4 N - 0.3867	4 C 0.7214	4 N 0.3051	4 N - 0.3813	4 N - 0.3466	4 N - 0.3824
5 C 0.7189	5 N - 0.3598	5 C 0.7254	5 C 0.7279	5 N 0.3030	5 C 0.7211
6 N - 0.3645	6 N 0.3051	6 N - 0.3537	6 N - 0.3934	6 C 0.6747	6 N - 0.3685
7 N - 0.3746	7 C 0.6239	7 N - 0.4315	7 N 0.0906	7 N - 0.3476	7 N 0.3054
8 N - 0.4932	8 N - 0.3472	8 N - 0.4854	8 C 0.2719	8 N - 0.2016	8 N - 0.0241
9 N 0.3048	9 N - 0.4917	9 C 0.3119	9 N - 0.4878	9 N - 0.3941	9 C - 0.3026
10 C 0.3087	10 C 0.3226	10 C 0.6236	10 N 0.3050	10 C 0.2831	10 N - 0. 4995
11 S 0.3257	11 S 0.3419	11 O - 0.4610	11 O - 0.4543	11 S 0.2138	11 O - 0.4507
12 C - 0.8109	12 C - 0.8153	12 O - 0.3532	12 O - 0.3518	12 C - 0.7343	12 O - 0.3528
13 O - 0.3557	13 Br 0.2363	13 O - 0.3074	13 O - 0.3078	13 N - 0.1393	13 O - 0.3097
14 O - 0.3125	14 O - 0.4622	14 S 0.4296	14 F - 0.1789	14 C 0.1410	14 O - 0.3718
15 O - 0.4638	15 O - 0.3555	15 C - 0.7018	15 S 0.4392	15 O - 0.4080	15 S 0.4369
	16 O - 0.3122	16 CL 0.3608	16 C – 0.7973	16 O - 0.3427	16 C - 0.7238
				17 O - 0.3018	17 H 0.3773

Bold type: The most positively and negatively charged centers.

2.1.5. Electronic spectrum

In this section, we obtained the infrared spectra (IR) and UV-Vi's spectrums of the derivatives of triazavirin, and to determine their stability, we drew the real part of the frequency vibrations. Fig. 6 shows the IR spectrum for TZV, TZV-Br, TZV-CL, TZV-F, TZV-NC and TZV-OH. The IR spectrum includes parameters such as frequency, ε (wave energy levels) and dipole strength (D). Absorption for TZV, TZV-Br, TZV-CL, TZV-F and TZV-NC occurs in the range of 500 – 3000 (cm^{-1}) and TZV-OH occurs in the range of 500 – 3500 (cm^{-1}) respectively. Also ,the maximum vibrational frequency for TZV, TZV-Br, TZV-Cl, TZV-F, TZV-NC and TZV-OH occurs in 1371.79 (cm^{-1}), 1370.69 (cm^{-1}), 1368.11 (cm^{-1}), 1370.61 (cm^{-1}), 1419.56 (cm^{-1}) and 1375.67 (cm^{-1}) respectively. Therefore, as the GNR and drug are combined, the maximum vibration frequency is reduced. With time-dependent density functional theory (TD-DFT), optimized gas-phase geometries were used to

calculate UV-Vis-Spectra, electronic transitions, vertical arousal energies, absorbances and the oscillator strength of the compounds. Fig. 7 illustrates the simulated UV spectrum of the compounds. Table 7 collects the most important molecular properties of the electronic spectrum.
The gas phase for the TZV, TZV-CL, TZV-Br, TZV-F, TZV-NC and TZV-OH compounds included the absorption band of UV spectra centering at 645.7, 772, 656.2, 685.8, 604.1 and 560.4 nm. HOMO-LUMO is close to TZV for the T-OH compound. It is appropriate to order atoms through electronegativity according to the periodic table from H to Br. The contribution to the transition of 645.7 nm from the HOMO to the LUMO results for TZV as can be seen from Table 7 with a 100 percent contribution. For H→L +1 transition, with 99 percent for the TZV-CL, is the largest contribution of 772nm. The TZV-Br is calculated at 656.2 nm with a transition of H→L +1 at 100 percent. The 99 percent H→L transition for the TZV-CL is calculated at 685.8 nm. With 66 percent H-1 →L transition is calculated for TZV-NC at 604.1 nm. The transition of H→L with 100% is calculated for the TZV-OH at 560.4 nm.

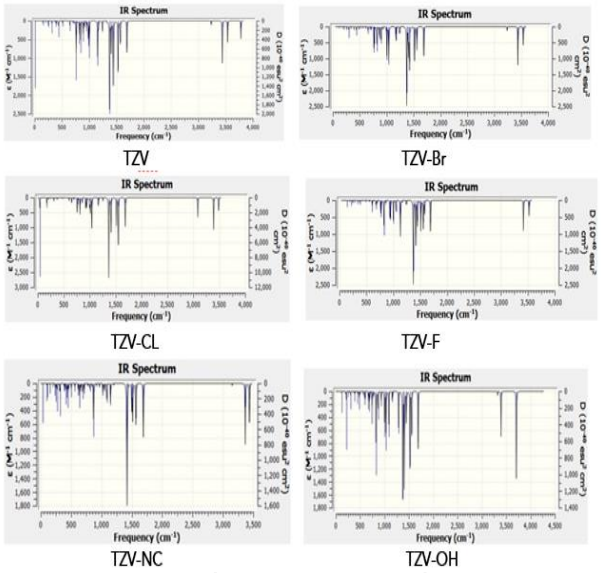

Figure 6. The infrared spectrums of the incident parameters versus the frequency, wave energy levels (ε) and dipole strength (D) of drugs.

Table 7. Computed excitation energy, wavelength and oscillator strength of the drugs.

Drugs	λ (nm)	E(λ) (eV)	f	Major contribution
TZV	645.7	1.92	0.0192	H→L (100%)
TZV-Br	656.2	1.89	0.0161	H→L+1 (100%)
TZV-CL	772	1.61	0.0316	H→L+1 (99%)
TZV-F	685.8	1.81	0.0331	H→L (99%)
TZV-NC	604.1	2.05	0.0006	H-1→L (66%)
TZV-OH	560.4	2.21	0.0143	H→L (100%)

3. Conclusion

In this work, triazavirin derivatives can easily be synthesized against new treatment with coronavirus. As inhibitors of COVID-19 along with DFT and TD-DFT in calculations of B3LYP/6-31G(d,p) basis set, Triazavirin (TZV) drugs have been studied. These parameters for unsubstituted TZV and derivatives of TZV are also computed by replacing H-atom by fluorine, chlorine, bromine, hydroxyl and cyanide group. The calculations of density functional theory have implemented to evaluate the current drug's thermal parameters, dipole moment, polarization, and molecular electrostatic potential. In addition, the Gaussian 09 program study, data showed that TZV-Br has the highest binding energy (1.215 eV) and could serve, compared to approved drug, TZV-OH and TZV-NC with binding energy 1.207 eV and 1.153 eV, as a good SARS-CoV-2 inhibitor. In addition, the other factors that could enhance binding energy might be high basicity (χ = 4.40 eV) and polarizing (α = 168.37 $bohr^3$) entirely functions as well as dipole moment (D = 13.34 Debye) of drug TZV-Br, instead of others. The density of states (DOS) was determined, and it allowed bettering describing the border orbitals. Thereafter, the calculated MEP maps show the positive potential sites are favorable for nucleophilic attack, whereas the negative potential sites are favorable for the electrophilic attack. It can be concluded that these parameters share the binding energy of these drugs together with different sizes in order to permit a certain degree of inhibition. All of these parameters could share the binding energy of these drugs in the active protein sites to a different extent. Finally, triazavirin could be considered as showing low binding against COVID-19 activity, meaning that further research is still needed to look at different sides of the proposed application of pharmacotherapy.

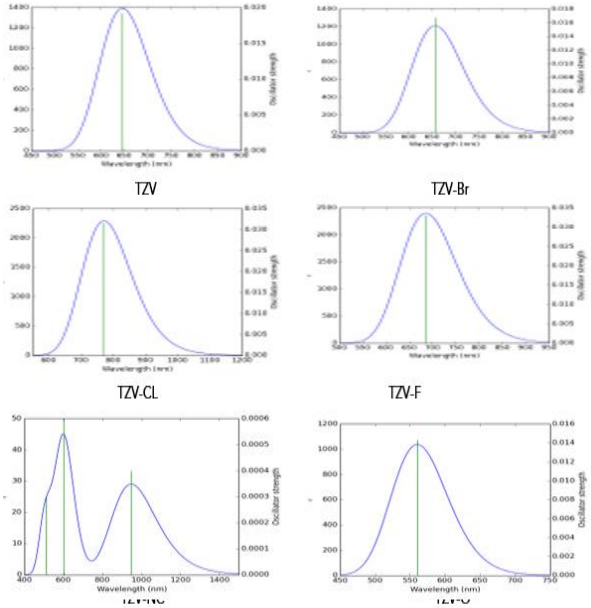

Figure 7. Simulated UV-vis spectra of the compounds.

Declaration of Competing Interest

The authors declare that they have no known competing financial interests or personal relationships that could have appeared to influence the work reported in this paper.

4. Acknowledgments

We show huge gratitude to Assist. Prof. Abbas Sh. Alwan for his precious assessing for this study. The authors are grateful to a department of physics, Thi-Qar University for their funding this study.

References

[1] M. Lipsitch, D. L. Swerdlow, and L. Finelli, "Defining the epidemiology of Covid-19—studies needed," *New England journal of medicine,* vol. 382, no. 13, pp. 1194-1196, 2020.

[2] M. Sun, J. Yang, Y. Sun, and G. Su, "Inhibitors of RAS might be a good choice for the therapy of COVID-19 pneumonia," *Zhonghua jie he he hu xi za zhi= Zhonghua jiehe he huxi zazhi= Chinese journal of tuberculosis and respiratory diseases,* vol. 43, pp. E014-E014, 2020.

[3] R. Hatada *et al.*, "Fragment molecular orbital based interaction analyses on COVID-19 main protease− inhibitor N3 complex (PDB ID: 6LU7)," *Journal of chemical information and modeling,* vol. 60, no. 7, pp. 3593-3602, 2020.

[4] K. Y. Wang *et al.*, "Structure of Mpro from COVID-19 virus and discovery of its inhibitors," *Nature,* vol. 582, no. 7811, pp. 289-93, 2020.

[5] H. Nishiura, N. M. Linton, and A. R. Akhmetzhanov, "Serial interval of novel coronavirus (COVID-19) infections," *International journal of infectious diseases,* vol. 93, pp. 284-286, 2020.

[6] D. Zhou, P. Zhang, C. Bao, Y. Zhang, and N. Zhu, "Emerging understanding of etiology and epidemiology of the novel coronavirus (COVID-19) infection in Wuhan, China," 2020.

[7] R. Yoshimura, N. Okamoto, Y. Kinishi, and A. Ikenouchi, "Absence of an association between serum interleukin-6 and brain-derived neurotrophic factor in drug-naïve first-episode major depression," *Archives of Clinical Psychiatry (São Paulo),* vol. 48, pp. 229-230, 2022, doi: https://doi.org/10.15761/0101-60830000000312.

[8] F. Wu *et al.*, "A new coronavirus associated with human respiratory disease in China," *Nature,* vol. 579, no. 7798, pp. 265-269, 2020.

[9] P. Zhou *et al.*, "Zhu Y, Li B," *Huang CL: A pneumonia outbreak associated with a new coronavirus of probable bat origin nature,* vol. 579, pp. 270-273, 2020.

[10] P. Zhou *et al.*, "A pneumonia outbreak associated with a new coronavirus of probable bat origin. Nature [Internet]. 2020; 579 (7798): 270–3," ed.

[11] J. A. Ruzicka, "Identification of the antithrombotic protein S as a potential target of the SARS-CoV-2 papain-like protease," *Thrombosis Research,* vol. 196, pp. 257-259, 2020.

[12] H. Lv, "protease inhibitors: A review of molecular selectivity and toxicity, HIV," *AIDS,* no. 7, p. 95.

[13] C. A. Devaux, J.-M. Rolain, P. Colson, and D. Raoult, "New insights on the antiviral effects of chloroquine against coronavirus: what to expect for COVID-19?," *International journal of antimicrobial agents,* vol. 55, no. 5, p. 105938, 2020.

[14] X. Wu *et al.*, "The efficacy and safety of Triazavirin for COVID-19: a trial protocol," *Engineering,* vol. 6, no. 10, pp. 1199-1204, 2020.

[15] M. Mohamed, F. Abrigach, S. El Kadiri, S. O. S. Hassane, M. H. Abdellattif, and R. Touzani, "Pyrazole, imidazole and triazole: In silico, docking and ADMET studies against SARS-CoV-2," *Materials Today: Proceedings,* 2022.

[16] I. Karpenko *et al.*, "Antiviral properties, metabolism, and pharmacokinetics of a novel azolo-1, 2, 4-triazine-derived inhibitor of influenza A and B virus replication," *Antimicrobial agents and chemotherapy,* vol. 54, no. 5, pp. 2017-2022, 2010.

[17] L. Sla, S. Borisevich, V. Rusinov, U. Ulomskiĭ, V. Charushin, and O. Chupakhin, "Investigation of Triazavirin antiviral activity against tick-borne encephalitis pathogen in cell culture," *Antibiotiki i khimioterapiia= Antibiotics and chemoterapy [sic],* vol. 59, no. 1-2, pp. 3-5, 2014.

[18] S. Y. Loginova *et al.*, "Investigation of prophylactic efficacy of Triazavirin against experimental forest-spring encephalitis on albino mice," *Antibiotiki i Khimioterapiia= Antibiotics and Chemoterapy [sic],* vol. 60, no. 5-6, pp. 8-11, 2015.

[19] O. Kiselev *et al.*, "A new antiviral drug Triazavirin: results of phase II clinical trial," *Voprosy virusologii,* vol. 57, no. 6, pp. 9-12, 2012.

[20] E. Tikhonova, T. Y. Kuz'mina, N. Andronova, O. Tyushevskaya, T. Elistratova, and A. Kuz'min, "Study of effectiveness of antiviral drugs (umifenovir, triazavirin) against acute respiratory viral infections," *Kazan medical journal,* vol. 99, no. 2, pp. 215-223, 2018.

[21] X. Wu *et al.*, "Efficacy and safety of triazavirin therapy for coronavirus disease 2019: a pilot randomized controlled trial," *Engineering,* vol. 6, no. 10, pp. 1185-1191, 2020.

[22] M. Voss and C. Currie, "Sleep Quality and the Importance Women Place on Healthy Eating Interact to Influence Psychological Resilience," *American Journal of Health Behavior,* vol. 46, no. 3, pp. 285-293, 2022, doi: https://doi.org/10.5993/AJHB.46.3.7.

[23] J. Zhang, "A study on impact of role of nutrition, Passolig system, and anti-doping law on the performance of Chinese athletes in sports," *Revista de Psicología del Deporte (Journal of Sport Psychology),* vol. 30, no. 3, pp. 296-305, 2021. [Online]. Available: https://www.rpd-online.com/index.php/rpd/article/view/499/175.

[24] D. Sudarman, D. Kartini, R. A. Helmi, and R. K. Dewi, "The Moderating Effect of Social-Media Among Managerial Capabilities and Strategic Innovations on Product Life Cycle Management and

Distribution Performance," *AgBioForum,* vol. 24, no. 2, pp. 83-95, 2022. [Online]. Available: https://agbioforum.org/menuscript/index.php/agb/article/view/129/78.

[25] S. Xavier, S. Periandy, and S. Ramalingam, "NBO, conformational, NLO, HOMO–LUMO, NMR and electronic spectral study on 1-phenyl-1-propanol by quantum computational methods," *Spectrochimica Acta Part A: Molecular and Biomolecular Spectroscopy,* vol. 137, pp. 306-320, 2015.

[26] O. Noureddine, N. Issaoui, and O. Al-Dossary, "DFT and molecular docking study of chloroquine derivatives as antiviral to coronavirus COVID-19," *Journal of King Saud University-Science,* vol. 33, no. 1, p. 101248, 2021.